REPORT

Characterization of recharge processes and groundwater flow paths using isotopes in the arid Santanghu basin, Northwest China

Ping Wang [1,2] · Feng'e Zhang [1] · Zongyu Chen [1]

Abstract

Isotopes and hydrochemistry were used to characterize the recharge and flow of groundwater in the arid Santanghu basin in Northwest China. The results of isotopic measurement and hydrochemical facies indicate that the predominant recharge mechanism is via rivers and streams. Modern recharge only occurs in the piedmont area of Moqinwula Mountains by ephemeral rivers, and the main recharge source is precipitation in the mountain areas at an elevation of about 2,200 m above sea level. Two recharge mechanisms were identified by stable isotope methods: the ephemeral stream recharge in the piedmont with the occurrence of evaporation during recharge, and subsurface inflow recharge from the mountain regions. Diffuse recharge derived from precipitation in the basin can be ignored because of the scarcity of precipitation and intense evaporation. Groundwater in the Paleogene and Neogene confined aquifers could represent recharge during cooler climatic conditions, rather than latitude or altitude effects, signified by tritium-free samples and significant depletion of heavy stable isotopes throughout the study area. Groundwater age data suggest that central faults are controlling the flow paths of the regional groundwater flow system. Groundwater moves from the piedmont plain to the basin lowland area through lateral flow, and changes flow direction to the spring zone of Hanshuiquan Oasis because of the barrier of the central faults. A conceptual model was defined, for better understanding of the groundwater recharge and flow systems. The major findings of this study have significant implications for groundwater protection and management in arid basins.

Keywords Arid regions · Environmental tracers · Groundwater recharge · Conceptual model · China

Introduction

For groundwater supply to be managed sustainably in water-scarce arid regions, understanding the sources of recharge and flow pattern of groundwater in these regions is imperative. Stable isotope techniques, hydrochemical techniques and numerical modeling methods have been commonly employed to identify groundwater recharge mechanisms and flow paths (Scanlon et al. 2002; Sophocleous 2005; Gates et al. 2008; Chen et al. 2012; Bourke et al. 2015). During the last three decades, the isotopic composition and chemical constituents of water have been widely used to characterize the groundwater recharge source, recharge rate and flow, and therefore address associated resource problems (Bajjali 2006; Edmunds et al. 2006; Zagana et al. 2007; Ma et al. 2013). Radioisotopes such as tritium (^{3}H) and radiocarbon (^{14}C) have been proven to be extremely useful in determining groundwater age and delineating flow paths, as well as in identifying the presence of modern recharge (Clark and Fritz 1997; Abbott et al. 2000; Scanlon et al. 2002; Chen et al. 2005).

The Santanghu basin is a recently explored coal-bearing and oil-gas-bearing basin in the water-scarce arid region of northwestern China (East-Central Asia). Groundwater is an important source of freshwater to meet the increasing demand for water supply due to the lack of reliable surface-water supplies. Sustainable development and management of groundwater requires knowledge of aquifer replenishment; however, only a few studies have been done on the hydrogeology since the investigation of groundwater resources in this basin began in 2010. Bai et al. (2015b)

✉ Feng'e Zhang
   feng_ezhang@163.com

1   Key Laboratory of Groundwater Sciences and Engineering, Ministry of Natural Resources. Institute of Hydrogeology and Environmental Geology, Chinese Academy of Geological Sciences, Zhonghua Bei Dajie, No. 268, Shijiazhuang 050061, People's Republic of China

2   China University of Geosciences, Beijing, Beijing 100083, People's Republic of China

present a study on the hydrogeological setting, and discuss the characteristics of aquifer storage. Li et al. (2015) studied the paleo-environment of groundwater in Easty Junggar Basin by isotopic and geochemical evidence and suggest that shallow groundwater was recharged under warm climate conditions in the Holocene, while deep groundwater was recharged in the cold period of late Pleistocene. To date, there has been little study on groundwater recharge and movement in this basin; hence, the focus of this study is to refine the hydrogeological conceptual models, and the overall goal is to offer some clues for sustainable utilization and protection of water resources. Two basic questions are considered for this: (1) What are the recharge mechanisms to aquifers? (2) How does the recharge water flow through the aquifers to the discharge area? In this paper, stable isotopes (δ^{18}O and δD) and hydrochemical composition were used to trace groundwater recharge and flow, and radiogenic isotopes (tritium, ^{3}H; and carbon-14, ^{14}C) were used to estimate groundwater ages. The paper presented a conceptual model to understand the recharge process and groundwater flow system in Santanghu basin, and the results may offer a better understanding of groundwater availability and protection in semi-arid and arid basins.

Study area

Geography and geology

The Santanghu basin, one of the subbasins of Junggar Basin in Xinjiang, NW China, is located at 43° 30′– 45° 10′ N, 91° 50′–94° 90′ E covering an area of about 24,000 km^2. It is a NW–SE-trending rift basin between the Tien Shan Mountains (Mts.) and the Altai Mts. (Fig. 1). Generally, the elevations of Tien Shan Mts. and Altai Mts. are 4,000–5,000 m above sea level (m asl) and 1,000– 3,000 m asl respectively. The south boundary of the basin is Moqinwula-Baiyi Mts., and the north boundary is Dahafutike-Huhongdelei-Suhaitu Mts. which are the boundary mountains between China and Mongolia. The elevation of the basin ranges from 468 to 1,800 m asl with a slope of 8.39–47.79‰ (Bai et al. 2015a). The minimum elevation is at the Hanshuiquan Oasis. Geographically, the basin consists of low mountains and hills and a pluvial plain. The climate is typical continental and arid with the mean annual temperature of 8.3 °C. Precipitation occurs fairly nonuniformly across the study area. The mean annual precipitation is about 41.6 mm in the basin, and more than 200 mm in the Moqinwula Mts., but 20–50 mm in the Baiyi Mts. The mean evaporation in the basin is about 2,273.7 mm (Bai et al. 2015a). All the surface water that enters the basin originates from the mountains; they are ephemeral rivers, recharged by snowmelt and rainfall in the mountain area. These rivers and streams disappear at

the pluvial piedmont plain when they flow into the basin. Four large ephemeral rivers, Toudaogou, Sandaogou, Sidaogou, and Toudaobaiyanggou, are from Moqinwula Mts. with annual average discharge of 1.69×10^6–3.94×10^6 m^3 (Bai et al. 2015a). However, they run dry by riverbed infiltration when they flow to about 1–2 km from the mountain pass.

The basement is composed of Precambrian and early Paleozoic fold belts, and is overlain by late Paleozoic, Mesozoic, and Cenozoic sedimentary strata (Chen et al. 2011). Permian and Jurassic formations are regarded as the major oil and gas reservoir, which is overlain by Paleogene, Neogene and Quaternary formations.

The Paleogene formation occurs in the Moqinwula pluvial plain, in the southeast of the study area, and is composed of sandstone, mudstone and glutenite with thickness of 100– 150 m (Fig. 2). The Neogene formation is widely distributed and consists of fluvial-clastic sedimentary with argillaceous sandstone, sandstone, mudstone, glutenite and conglomerate. Its thickness increases from <50 m at the mountain front to about 50–100 m in the center of the basin. The Quaternary formation, overlying the Neogene, consists of boulders, pebbles and gravel in the pluvial plain, and sand interbedded with clay in the pluvial-alluvial plain. The thickness is about 100–250 m in the piedmont and decreases to about 10 m in the basin.

Two buried faults, the central fault (F1) and Hanshuiquan-Laoyemiao fault (F2), occur in the basin (Fig. 1). The F1 is a thrust fault running NW–SE and dipping in the NE, and it is a compressive fracture; thus, the material in the fault zone is fine and it is a compact structure with different degrees of water resistance. F2 is a high thrust fault running W–E and dipping in the south. The data of geological exploration showed that the surface layer near F1 and F2 is loose deposit and it is thin and permeable. The underlying confined aquifers (Neogene and Paleogene) north and south of the faults showed completely different water abundance in pumping tests. The results suggested that both faults act as barriers which may block the lateral flow from the piedmont area (Bai et al. 2015a).

Hydrogeology

Three aquifers occur in the study area: Quaternary (Q), Neogene (N) and Paleogene (P). The Quaternary aquifer is an unconfined aquifer which mainly exists in the piedmont of Moqinwula Mts. with a thickness of 100–120 m, and the Hanshuiquan Oasis with a thickness of 10–30 m. The Quaternary formation in the rest of the studied area is a permeable layer without water storage. The Neogene aquifer is a confined aquifer which is widely distributed in the basin below the depth 93–102 m and consists of sandstone and argillaceous sandstone with a thickness of 30–92 m. The Paleogene formation in the southeast of the
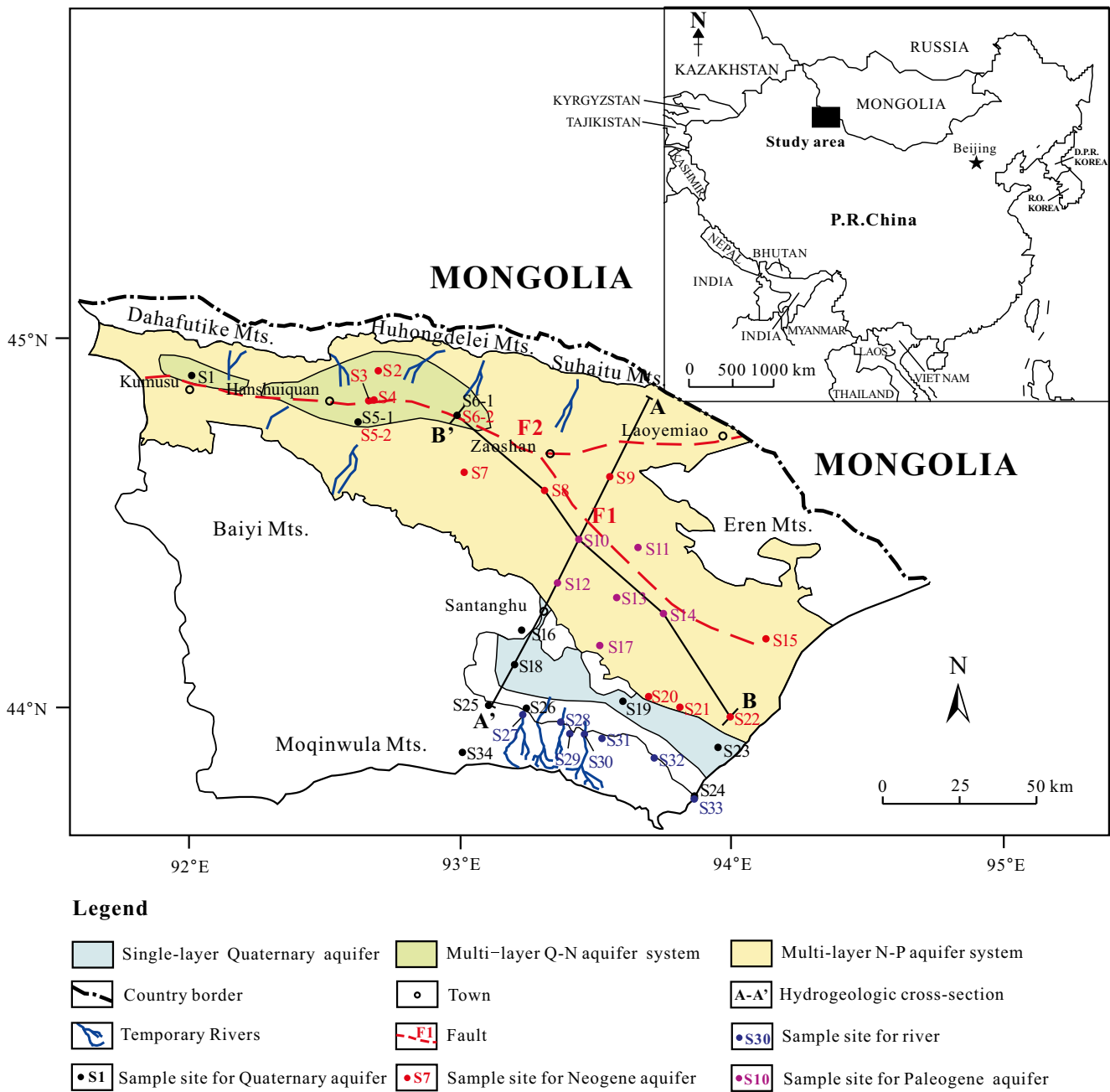
Fig. 1 Study area and sample sites

study area is composed of sandstone, mudstone and glutenite, with thickness of 51–100 m.

The aquifer system consists of a single-layer system and multi-layer system (Fig. 1). The single-layer system is a Quaternary aquifer with a thickness of 100–120 m, consisting of gravel and sand. It is distributed locally in the piedmont alluvial fan of Moqinwula Mts. (Fig. 1). The aquifer deposits are coarse-grained pebbles and gravel in the foothills, and sand in the distal fan. Correspondingly, the hydraulic conductivity ranges from 3 to 25 m/day, and depth to the water-table ranges from 1 to 70 m. The total dissolved solids (TDS) of water varies from <1,000 to 2,164 mg/L.

The multi-layer arrangement presents two types of aquifer system: the Neogene-Paleogene aquifer system (N-P) and the Quaternary-Neogene aquifer system (Q-N).

The N-P aquifer system is regionally distributed within the basin, and consists of the Quaternary aquifer, Neogene aquifer and Paleogene aquifer. The Quaternary formation overlies the N-P aquifer, and is an unsaturated layer without water storage, with a thickness less than 20 m. The Neogene aquifer is distributed in the piedmont of Baiyi Mts. and the North Mts., and the Paleogene aquifer occurs in the Moqinwula pluvial plain in the southeast of the
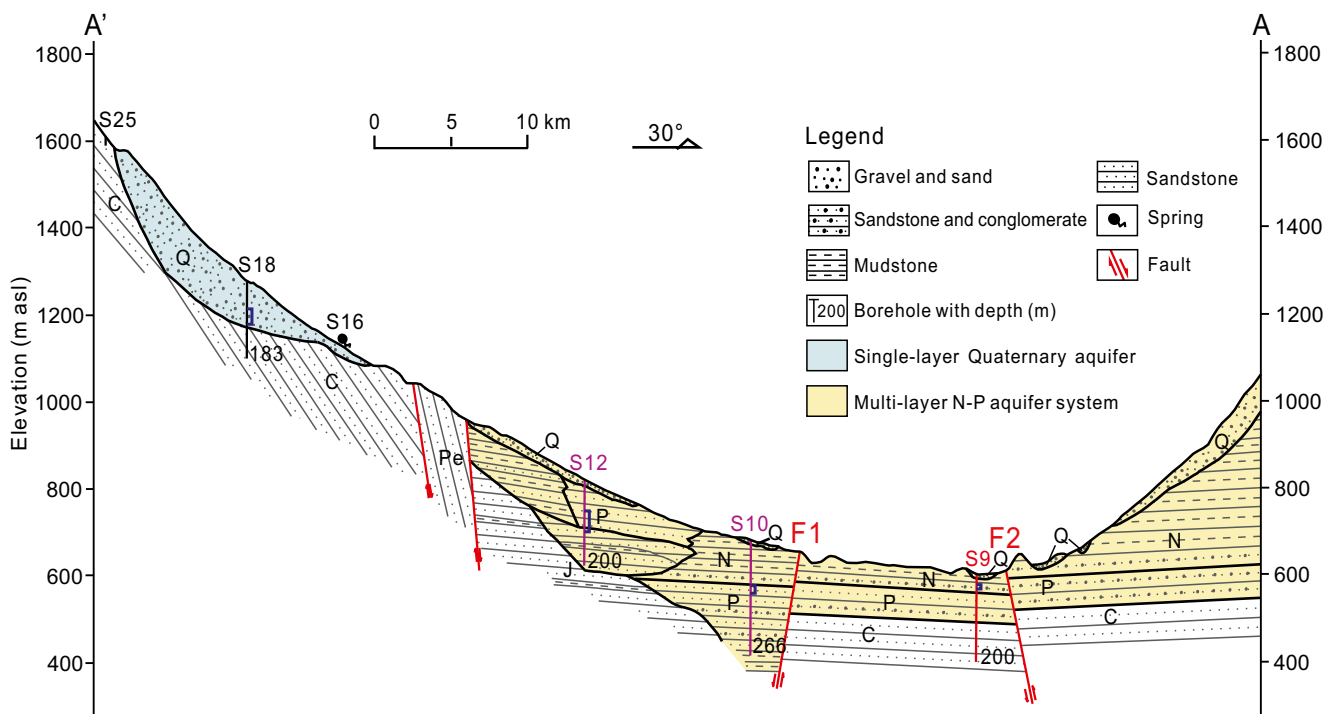
Fig. 2 Hydrogeologic cross section along the transect A–A′. Q Quaternary, N Neogene, P Paleogene, J Jurassic, Pe Permian, C Carboniferous

study area. These aquifers are composed of glutenite and sandstone, with a total thickness of 51–100 m. The hydraulic conductivity ranges from 0.14 to 4.8 m/day, while the hydraulic head of boreholes is from +1.0 to +83.4 m above the surface. The TDS of water is 790–2,180 mg/L. The aquitards are composed of mudstone and distributed continuously within the aquifer system.

The Q-N aquifer system occurs merely around Hanshuiquan in the centre of the basin (Fig. 1). The overlying Quaternary unconfined aquifer is composed of sand with a thickness of 10–30 m and hydraulic conductivity <3 m/day. Depth to the water table is about 3 m and the TDS of the water is about 2,000 mg/L. The underlying Neogene aquifer consists of sandstone and argillaceous sandstone with a thickness of 30–92 m. The hydraulic conductivity ranges from 0.25 to 3.27 m/day. The hydraulic head of boreholes is from +0.2 to +33.8 m above the surface and the flow rate ranges from 1.35 to 4.42 L/s. The TDS of water is 1,000–2,000 mg/L. There is a close hydraulic connection between the overlying Quaternary aquifer and Neogene aquifer since the aquitard distributes discontinuously.

Materials and methods

A total of 36 water samples were collected for isotope and hydrochemistry measurement (Fig. 1), including 7 river water samples and 29 groundwater samples. Groundwater was sampled from springs, boreholes/wells and dug wells. Samples from wells were collected after pumping until the flowing water showed a stabilized temperature, pH, and electrical conductivity (EC). Physical and chemical parameters such as water temperature and pH, were measured immediately in the field. Samples for stable isotopes D and ^{18}O were collected in 0.5-L glass bottles or high-density polyethylene plastic with gas-tight caps. Similarly, ^{3}H samples were collected in 0.5–1-L high-density polyethylene plastic bottles with gas-tight caps. The dissolved inorganic carbon (DIC) for ^{14}C determination was extracted as $BaCO_3$ from 120 L of groundwater by adding $BaCl_2$ and CO_2-free NaOH until pH 12.

Isotopic analyses using standard methods were performed by the Key Laboratory of Groundwater Sciences and Engineering, Ministry of Natural Resources, China. The δ^{18}O value was determined using CO_2–H_2O equilibration-mass spectrometry, while the δD value was determined using H_2–H_2O equilibration-mass spectrometry under the catalysis of platinum, followed by analysis with a MAT253 gas isotope mass spectrometer. The isotope results were reported as relative (per mil) deviation from the isotopic ratio of the sample. The uncertainty (2σ) for δ^{18}O and δD values were ±0.1 and ±1‰, respectively.

Tritium (^{3}H) and ^{14}C were used to identify the age or residence time of groundwater. The tritium was determined after water samples were electrolytically enriched, using a 1220 Quantulus ultra-low background liquid scintillation spectrometer. The results were reported as tritium units with a typical

error of ±0.5 TU, and the lower detection limit for tritium was 1 TU. The ^{14}C of DIC was determined radiometrically by liquid scintillation counting (1220 Quantulus) after conversion to benzene. The specific ^{14}C activity was reported in the unit of percent modern carbon (pMC).

Results

Isotopes in precipitation and surface water

The isotopic signature of precipitation can provide information on the origin and movement of groundwater. No samples of precipitation were obtained due to small precipitation in the studied basin in the study period (2010–2011). The data sets (1986–2002) of the GNIP (Global Network on Isotopes in Precipitation) station of Urumqi (87° 37′ E, 43° 47′ N, 918 m asl) which is about 300 km from the studied area, may be used to characterize the isotopic signature of local precipitation. The local meteoric water line (LMWL) fitted using monthly δD and $\delta^{18}O$ by the least square method, was $\delta D = 6.97\delta^{18}O + 0.12$ ($n = 119$, $R^2 = 0.94$) (Zhang et al. 2008). The weighted mean value of δD and $\delta^{18}O$ is −74.2 and −10.8‰, respectively.

It should be noted that the precipitation in mountain areas is more plentiful than that in the basin. The altitude of maximum precipitation zone is 1,500–2,000 m asl in winter and about 5,000 m asl in summer. Thus, the LMWL from Urumqi could not well represent the isotopic signature of high mountain precipitation. A previous study (Kreutz et al. 2003) has found a distinct shift of the LMWL of Tien Shan Mts. from the Global Meteoric Water Line (GMWL); the slope of LMWL in the area of altitude 5,100 m asl was about 6.9, but the mean d-excess was about 23‰, which reflected the contribution of local water vapor of the inland arid zone to precipitation. Thus, the LMWL of the mountain areas should be plotted above the LMWL of Urumqi in the δD–$\delta^{18}O$ plot.

Seven samples of river water (Table 1, Nos. S27–S33) collected at the mountain-pass valleys of Moqinwula Mts. may be used to characterize the surface water in the mountain area. The isotope ratio of these samples varied from −101 to −73‰ with a mean value of −89 ± 9‰ for δD, and from −15.7 to −11.4‰ with a mean value of −13.9 ± 1.3‰ for $\delta^{18}O$. The content of ^3H was about 17–37 TU with a mean value of 28 ± 6 TU, and the d-excess ranged from 18.2 to 24.6‰ with a mean value of 22.2‰. The fitting line of δD–$\delta^{18}O$ was $\delta D = 6.79\ \delta^{18}O + 5.36$ ($n = 7$, $R^2 = 0.98$), which is quite similar to the LMLW of Tien Shan Mts. given by Kreutz et al. (2003). Thus, the isotope signature of these surface-water samples should represent the recharge from rivers in the mountain area, and the fitted line

was named "regional recharge water line (RRWL)" in order to distinguish the LMWL (Fig. 3).

Isotopes in groundwater

The stable isotopic ratios of water samples in the Quaternary aquifer varied from −104 to −81‰ with a mean value of −93.5 ± 6.7‰ for δD, and −14.4 to −10.9‰ with a mean value of −12.9 ± 1.3‰ for $\delta^{18}O$. The δD and $\delta^{18}O$ value of samples from the Neogene confined aquifer ranged from −96 to −80‰ (mean value −89.9 ± 4.6‰) and from −13.6 to −10.0‰ (mean value −11.9 ± 1.1‰), respectively. Those samples of Neogene aquifer in the Q-N system had values of −91 to −80‰ for δD, −11.5 to −11.1‰ for $\delta^{18}O$, respectively. While those in the N-P system had values of −96 to −92‰ for δD, −13.6 to −10.0‰ for $\delta^{18}O$, respectively. The stable isotopic ratio of water in the Paleogene aquifer was from −112 to −102‰ (mean value −109 ± 3.5‰) for δD, and from −14.7 to −13.9‰ (mean value ~14.3 ± 0.3‰) for $\delta^{18}O$.

Tritium contents of most groundwater samples were less than 3 TU. Six samples (Nos. S16, S18, S23–S25, S34) contained tritium contents of 5–34 TU. All these groundwaters were emerging in the piedmont of Moqinwula Mts., expect sample No. S34.

^{14}C activity of groundwater in the Quaternary aquifer ranged from 11.2 to 86.6 pMC, while it was 6.7–79.9 pMC in the Neogene aquifer and 19.7–80.9 pMC in the Paleogene aquifer. For the Quaternary aquifer, those samples with ^{14}C activity >44 pMC were collected from the piedmont of Moqinwula Mts. (Nos. S16, S18–S19, S23–S24, S34), and those with ^{14}C activity <16 pMC were from Hanshuiquan Oasis (Nos. S1, S5-1, S6-1). For the confined aquifers (Neogene and Paleogene), relatively high ^{14}C activity samples (>41 pMC) in both aquifers occurred close to the south mountains (Nos. S12, S17, S22).

Hydrochemistry

Water quality in the study area can be categorized into two main types as shown in Fig. 4: SO_4-HCO_3/HCO_3-SO_4 type and Cl-SO_4 type. The surface water from the Moqinwula Mts. is characterised by SO_4-HCO_3 or HCO_3-SO_4 type with TDS less than 1,000 mg/L (Nos. S27, S28, S31, S33). The groundwater of the Quaternary aquifer generally contains TDS from less than 700 mg/L in the piedmont of Moqinwula Mts. (Nos. S16, S18–S19, S23–S24, S26) to 4,950 mg/L near Hanshuiquan (No. S5-1). Evolution of water chemistry is characterised by increasing concentration of SO_4 and Cl along the regional groundwater flow path, from recharge area to discharge area, i.e. in the southern part of the basin, groundwater is chemically of the SO_4-HCO_3 or HCO_3-SO_4 type with TDS <700 mg/L in the piedmont area of Moqinwula Mts., but it changes to Cl-SO_4 type with TDS >490 mg/L (Nos. S3, S4,

Table 1 Analytical results for water samples. *Q* Quaternary; *N* Neogene; *P* Paleogene

| Sample No.	Elevation (m asl)	Sample date	Depth (m)	Type	Aquifer	Temp (°C)	pH	δD (‰)	$\delta^{18}O$ (‰)	^3H (TU)	K^+ (mg/L)	Na^+ (mg/L)	Ca^{2+} (mg/L)	Mg^{2+} (mg/L)	Cl^- (mg/L)	SO_4^{2-} (mg/L)	HCO_3^- (mg/L)	TDS (mg/L)
S1	703.3	2011/8/23	20.3	Well	Q	14	7.8	−98	−12.3	3	5.2	624.9	224.7	63.8	515.5	1,221.0	142.0	2,754
S2	542.0	2011/9/29	137.8	Well	N	21	7.9	−82	−11.5	3	3.9	324.4	184.7	62.3	206.4	993.1	88.4	1,848
S3	470.6	2011/10/4	78.0	Well	N	13	8.0	−80	−11.1	1	9.5	5,020	726.9	169.1	4,648.4	5,623.2	193.0	16,294
S4	475.0	2011/10/4	68.2	Well	N	13	7.6	−86	−11.2	1	8.8	1,863.5	328.0	49.2	1,673.6	2,221.8	112.1	6,201
S5–1	521.1	2011/8/27	22.9	Well	Q	13	7.9	−92	−11.0	2	7.4	1,499.4	249.0	40.8	1,428.2	1,611.9	122.0	4,947
S5–2	521.1	2011/8/27	89.8	Well	N	13	7.9	−91	−11.1	2	8.3	1,931.4	252.2	47.4	1,816.6	2,082.6	112.1	6,250
S6–1	555.5	2011/8/18	8.6	Well	Q	14	7.9	−93	−11.4	3	4.7	466.8	217.8	35.4	290.0	1,111.9	72.2	2,197
S6–2	555.5	2011/8/22	95.0	Well	N	14	7.9	−89	−11.1	2	21.1	915.2	426.7	101.4	694.9	2,188.0	99.6	4,418
S7	664.7	2011/5/21	43.1	Well	N	3	7.7	−92	−11.5	3	5.1	833.0	110.7	10.7	629.7	1,008.1	222.9	2,725
S8	655.7	2011/7/15	66.9	Well	N	14	8.2	−93	−11.5	1	5.7	558.4	105.6	31.4	508.6	716.9	114.6	2,024
S9	599.4	2011/4/7	21.0	Well	N	12	7.8	−92	−10.0	1	5.3	1,866.0	197.2	38.1	1,879.2	1465.7	137.0	5,725
S10	683.4	2010/12/11	74.4	Well	P	14	7.7	−109	−14.5	3	3.5	217.2	111.4	26.6	142.1	524.4	157.0	1,125
S11	711.8	2011/6/8	41.9	Well	P	10	8.3	−111	−13.9	2	2.9	627.2	87.4	21.7	604.1	717.1	142.0	2,180
S12	827.9	2010/11/26	73.1	Well	P	9	7.5	−106	−14.5	3	2.9	191.9	114.6	27.8	95.9	461.7	299.1	1,068
S13	796.2	2011/5/11	25.1	Well	P	13	7.7	−112	−14.7	2	2.6	269.7	77.9	19.9	112.0	514.7	174.3	1,104
S14	748.6	2011/6/13	50.3	Well	P	14	8.7	−111	−14.5	2	1.4	300.6	18.7	5.5	181.9	293.1	154.4	925
S15	566.3	2011/5/9	54.5	Well	N	12	8.3	−93	−13.6	3	2.6	533.3	35.7	2.4	311.1	653.5	158.2	1,648
S16	1101.5	2011/12/10	Surface	Spring	Q	3	7.8	−101	−14.4	20	2.4	116.2	79.6	19.3	43.9	201.4	299.1	647
S17	1045.5	2011/5/7	67.6	Well	P	15	7.4	−102	−13.9	2	2.0	181.6	73.0	17.9	106.4	290.4	205.5	796
S18	1283.3	2010/12/19	64.5	Well	Q	13	7.6	−104	−14.2	5	3.7	81.8	59.8	12.1	43.9	147.4	211.9	475
S19	1339.0	2011/7/20	45.4	Well	Q	14	8.2	−81	−13.2	1	1.4	50.2	28.5	9.3	22.7	83.8	137.0	295
S20	1151.1	2011/12/13	18.3	Well	N	3	8.2	−92	−13.6	2	1.0	56.4	24.6	7.5	21.5	83.8	112.1	273
S21	1033.7	2011/5/26	36.6	Well	N	9	8.5	−96	−13.4	2	1.1	98.7	19.9	5.1	56.3	76.2	118.3	367
S22	768.7	2011/4/24	60.3	Well	N	14	7.4	−93	−13.0	2	2.5	63.4	94.3	23.4	31.2	204.1	231.6	557
S23	1070.8	2010/12/30	45.0	Well	Q	14	8.0	−98	−14.2	24	2.3	19.1	35.9	5.3	14.7	27.1	137.1	191
S24	2060.0	2011/10/15	4.6	Well	Q	12	8.1	−91	−13.5	34	0.9	14.4	49.1	7.7	12.9	58.5	138.2	227
S25	1603.2	2010/12/2	0.9	Dug well	Q	9	8.1	−83	−10.9	13	1.0	19.3	28.7	4.5	12.2	37.3	100.9	167.39
S26	1665.0	2011/9/17	Surface	Spring	Q	9	–	−92	−14.4	4	–	–	–	–	–	–	–	–
S27	–	2011/9/17	Surface	River		10	8.0	−93	−14.3	17	2.2	86.3	85.6	31.4	57.1	215.7	261.7	609
S28	–	2011/9/17	Surface	River		10	8.1	−97	−15.1	23	2.1	40.5	83.6	20.5	22.0	107.7	286.6	420
S29	–	2011/9/17	Surface	River		9	–	−101	−15.7	25	–	–	–	–	–	–	–	–
S30	–	2011/9/17	Surface	River		9	–	−92	−14.2	28	–	–	–	–	–	–	–	–
S31	–	2011/9/17	Surface	River		10	8.3	−80	−12.9	32	2.0	26.9	71.6	13.3	14.7	125.5	163.3	339
S32	–	2011/9/17	Surface	River		9	–	−73	−11.4	37	–	–	–	–	–	–	–	–
S33	–	2011/9/22	Surface	River		7	8.1	−88	−13.8	31	1.9	8.9	47.8	7.2	9.5	43.1	137.1	187
S34	1761.8	2010/12/2	1.8	Well	Q	10	8.3	−96	−12.9	7	6.0	441.8	201.1	62.2	346.2	911.9	232.9	2,164
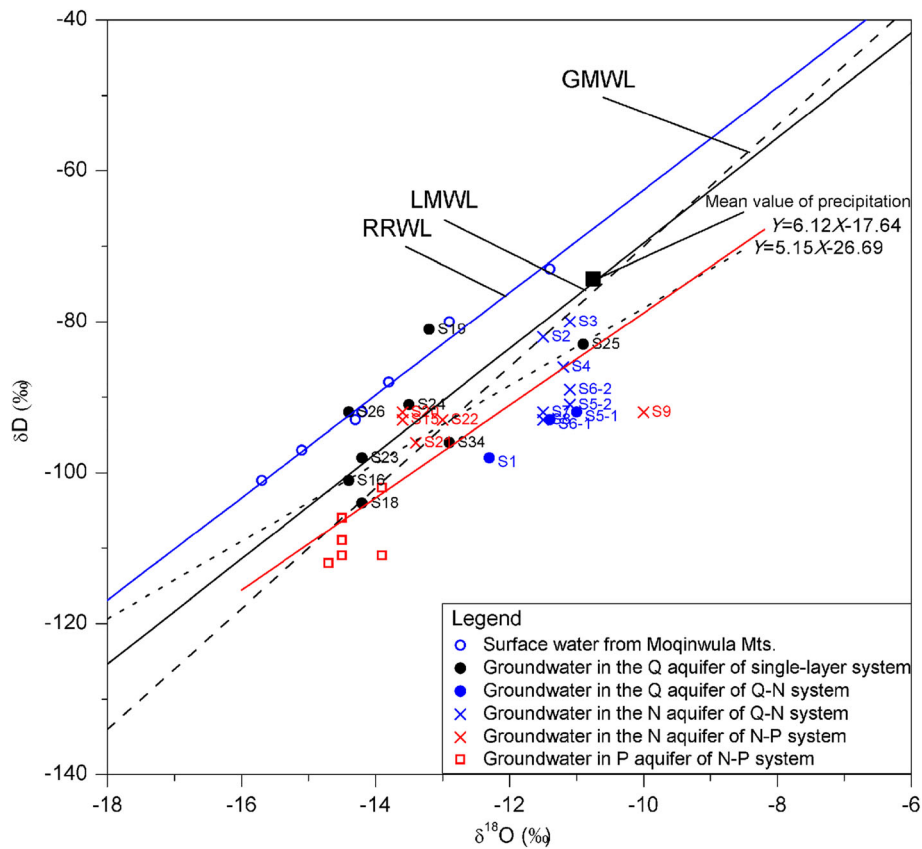
Fig. 3 Plot of δD versus δ^{18}O for groundwater in the aquifers. GMWL Global Meteoric Water Line; LMWL local meteoric water line; RRWL regional recharge water line; the black dotted line is the fitting line ($Y = 5.15X - 26.69$) of groundwater samples in the Q aquifer of the single-layer system except for samples Nos. S19, S25 and S26; the red solid line is the fitting line ($Y = 6.12X - 17.64$) of samples from the N aquifer and P aquifer except for samples Nos. S9, S11 and S15

S5-1, S5-2) by increasing SO_4 and Cl concentrations towards the discharge area near Hanshuiquan. The hydrogeochemistry evolving trend is consistent with that of East Junggar Basin reported by Li et al. (2015) and is similar with other arid regions.

Discussion

Groundwater age

Tritium has often been used to estimate the residence time of young groundwater in shallow groundwater systems (Clark and Fritz 1997; Małoszewski and Zuber 1982). Generally, groundwater containing tritium of more than 3 TU indicates that it was recharged after 1953 (the period of nuclear testing). Nowadays, in some places, the tritium content in the atmosphere has gradually reduced to natural levels, and in that case the residence time estimation based on tritium content could be doubtful. However, at Urumqi, the tritium level in precipitation was still relatively high with an average tritium content of about 30 TU, thus the tritium can still be used to estimate the residence time of groundwater here. The input function of

precipitation is required for such estimation. The tritium time series were reconstructed by using the data sets (1986–2002) of Urumqi station from the GNIP. Tritium contents in precipitation during 1953–1959 were approximated from correlation with the data of Ottawa, Canada, while the values during the period of 1960 to 1986 were estimated by the Doney method (Doney et al. 1992).

The decay paths for groundwater samples with 3, 10, 15 and 40 TU in 2011 are shown as solid lines in Fig. 5. A sample containing tritium at content less than 3 TU indicates recharge prior to 1953. A sample with 3–10 TU indicates water recharge in 1953–1960 and a sample with 10–15 TU indicates water recharge in 1971–2000, while a sample with 15–40 TU probably indicates water recharge in 2000–2011 or 1966–1971. A sample containing tritium at concentrations greater than 40 TU indicates water was recharged from precipitation in 1962–1966.

According to the aforementioned classification, those six samples (Nos. S16, S18, S23–S25, S34) with tritium contents >3 TU should have recharged after 1953 and have residence time less than 65 years. The groundwater of sample Nos. S18 and S34 has residence time of 58–65 years and was recharged in 1953–1960, and the groundwater of No. S25 has residence
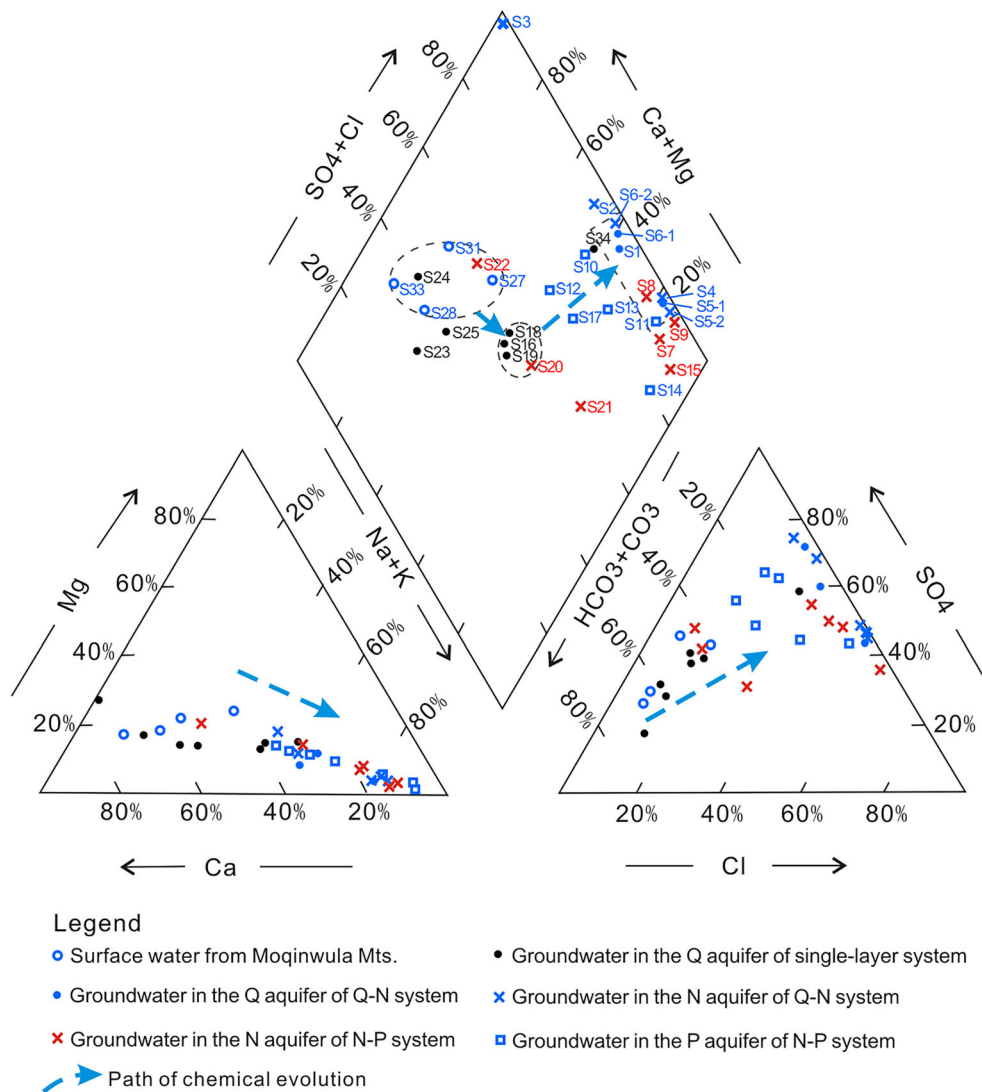
Fig. 4 Piper diagram of groundwater and river water samples

time of 18–47 years which was recharged in 1971–2000. The groundwater of Nos. S16, S23, S24 has residence time of 47–52 years or 7–18 years and may have been recharged in 1966–1971 or 2000–2011.

The samples with tritium <3 TU were presumed to be recharged before 1953. Their ages were determined by ^{14}C dating methods. For the ^{14}C dating of groundwater, the initial input ^{14}C activity (A_0), which is assumed to be 100 pmC, is usually diluted by low ^{14}C activity carbon sources during physical or chemical processes in the aquifer. Thus, it should be corrected before being used to estimate the groundwater age. There are several methods to correct the initial ^{14}C activity for dead-C dilution (Clark and Fritz 1997). These methods consider either only chemical mixing between the carbon compounds and/or isotopic fractionation. Some models rely on water chemistry, including the alkalinity model (Tamers 1975) and chemical mass balance model (Clark and Fritz 1997),

while other models use the δ^{13}C value of the DIC to estimate the contribution of dissolved calcite to the DIC load (Pearson and Hanshaw 1970). In this work, ^{14}C dating methods related to the stable isotope ratio δ^{13}C can not be used because δ^{13}C data are not available. The methods used in this study include the statistical methods (Vogel 1970), Tamers model (Tamers 1975), and ^{3}H correction method.

A first attempt to understand the ^{14}C age of groundwater was undertaken using a statistical method (Vogel 1970). Sample Nos. S12 and S22 have tritium content <3 TU and ^{14}C activity >80 pMC; thus, that value (80% A_0) was assumed to be the initial ^{14}C activity (A_0) and used to estimate groundwater age by the Vogel method. Secondly, in an alternative approach, the Tamers model (Tamers 1975), which assumes that DIC does not exchange with carbonate sediments, was used for ^{14}C dilution correction. In this case, about 50% input of the carbon
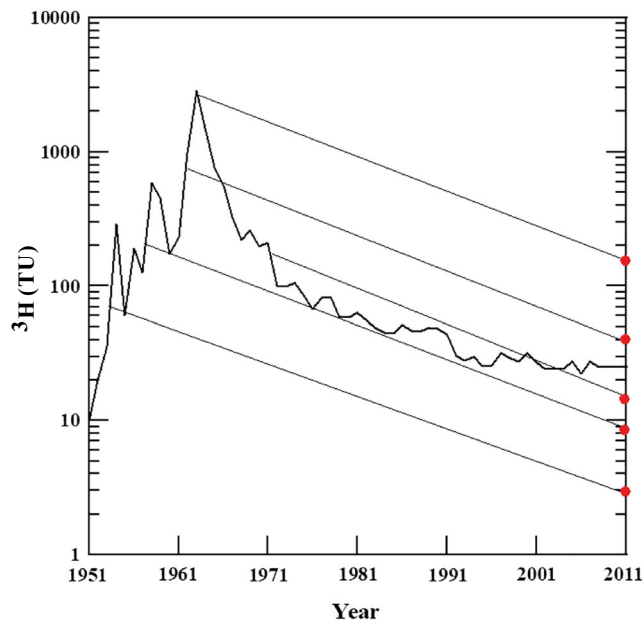
Fig. 5 The tritium time series in precipitation at Urumqi station

in DIC ($A_0 \approx 50$ pMC) is derived from soil carbon dioxide and the other half from dissolving carbonate minerals. Another independent approach for A_0 estimation is the use of a ^{14}C-^{3}H plot by extrapolating the fitting line to the detection limit of ^{3}H (Verhagen et al. 1974). In the present work, those samples with ^{14}C activity >60 pMC were used to make the ^{14}C-^{3}H plot, and the fitting line of samples is $Y = 0.15X + 74.62$. And the initial ^{14}C activity (A_0) was at about 74.6 pMC after extrapolating the line to the detection limit of ^{3}H (about 1 TU).

Groundwater ages determined by those methods are listed in Table 2 with the mean corrected ages of these three approaches, in which the age "modern" means that the groundwater was recharged after 1950. The estimated ages both from the Tamers model and the ^{14}C-^{3}H plot are not far from those given by the Vogel method. The ^{3}H corrected age lies between the statistical method and Tamers model, which should be close to the real groundwater age, since the Tamers model simply assumed ^{14}C dilution from a pure chemical dissolution of carbonate minerals.

Table 2 Groundwater ages determined by application of ^{14}C-DIC models. *Q* Quaternary; *N* Neogene; *P* Paleogene

| Sample No.	Type	Aquifer	^{14}C (pMC)	^{3}H (TU)	HCO$_3$ (mg/L)	Uncorrected age(years BP)	Vogel model age(years BP)	Tamers model age(years BP)	^{3}H corrected age(years BP)	Mean age(years BP)
S1	Well	Q	11.2	3	141.96	18,069	16,224	12,652	15,647	14,841
S2	Well	N	22.7	3	88.42	12,255	10,410	6,772	9,832	9,005
S5–1	Well	Q	15.4	3	122.04	15,471	13,627	10,047	13,049	12,241
S5–2	Well	N	14	2	112.08	16,230	14,386	10,768	13,808	12,987
S6–1	Well	Q	15.5	3	72.23	15,407	13,562	9,967	12,985	12,171
S7	Well	N	6.72	3	222.91	22,322	20,477	17,172	19,899	19,183
S8	Well	N	22.5	1	114.57	12,328	10,483	6,752	9,905	9,047
S9	Well	N	14.78	1	136.98	15,806	13,961	10,462	13,383	12,602
S10	Well	P	40.3	3	157.03	7,521	5,677	2,252	5,099	4,342
S11	Well	P	19.7	2	141.96	13,413	11,569	7800	10,991	10,120
S12	Well	P	80.9	3	299.11	1,756	−88	Modern	−666	Modern
S15	Well	N	9.59	3	158.15	19,382	17,537	13,761	16,959	16,086
S16	Spring	Q	81	20	299.11	1,559	−285	−3,709	−863	47–52(MRT-3H)
S17	Well	P	50.5	2	205.47	5,653	3,808	649	3,230	2,562
S18	Well	Q	49.1	5	211.87	5,887	4,042	636	3,465	58–65(MRT-^{3}H)
S19	Well	Q	44.1	1	136.98	6,766	4,922	1,165	4,344	3,477
S20	Well	N	37.1	2	112.08	8,206	6,361	2,638	5,784	4,928
S21	Well	N	17.5	2	118.3	6,847	5,003	1,199	4,425	3,542
S22	Well	N	79.9	2	231.63	1,855	10	Modern	−567	Modern
S23	Well	Q	68.2	24	137.09	3,165	1,320	Modern	743	47–52(MRT-3H)
S24	Well	Q	86.6	34	138.23	1,190	−654	Modern	−1,232	47–52(MRT-3H)
S25	Dug well	Q	44.5	13	100.87	6,694	4,849	Modern	−666	18–47(MRT-^{3}H)
S34	Well	Q	64.63	7	232.87	3,608	1,764	Modern	1,186	58–65(MRT-^{3}H)
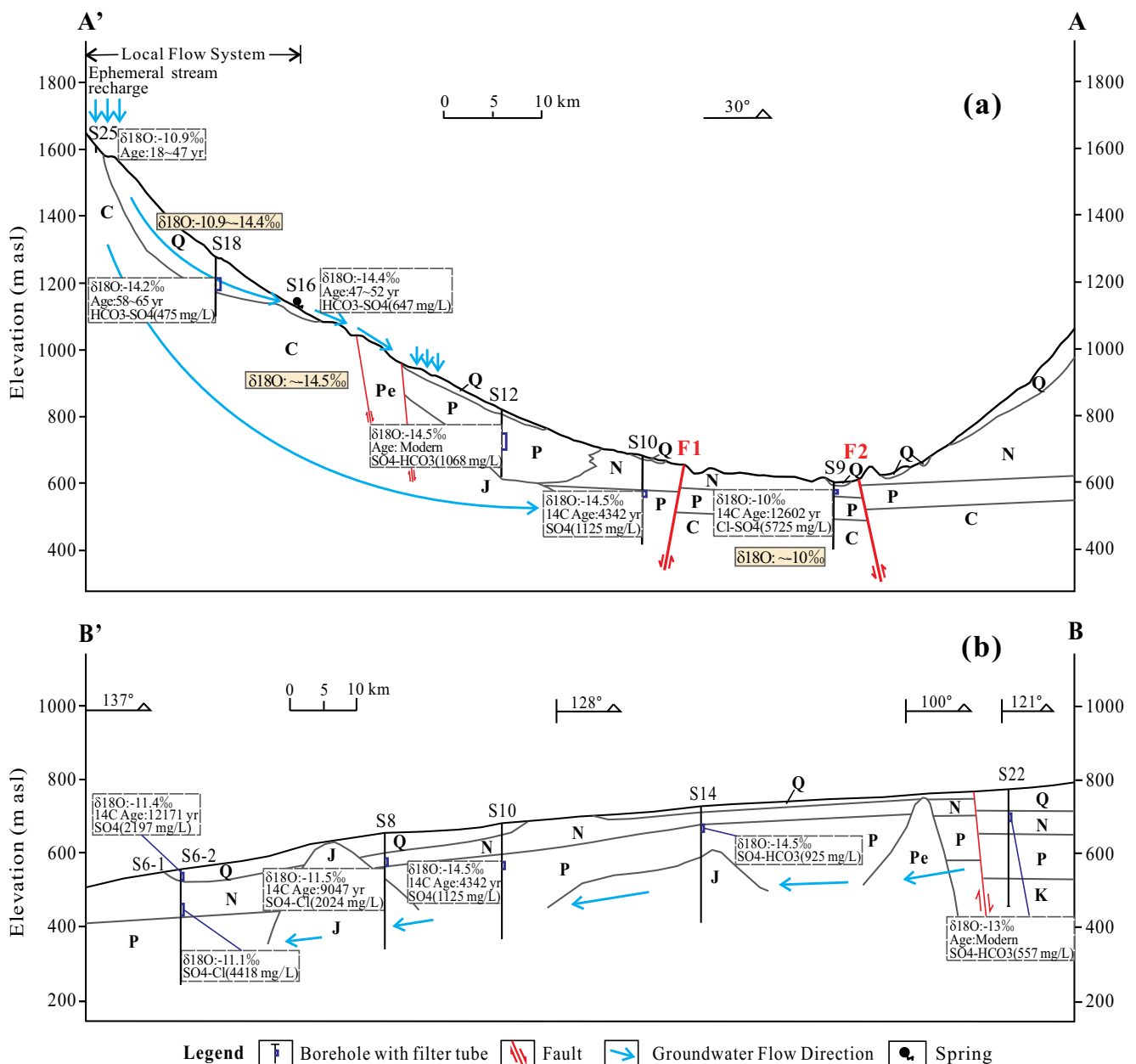
Fig. 6 Flow path of groundwater along: **a** the A–A′ transect; **b** the B–B′ transect. Q Quaternary, N Neogene, P Paleogene, J Jurassic, Pe Permian, C Carboniferous, K Cretaceous

The results of age estimation suggested that young groundwater with age <65 years mainly occurs in the aquifer of the single-layer system. Groundwater in the aquifers of the Q-N system has an age range of 12–14 ka and 9 ka BP for the Quaternary aquifer and Neogene aquifer, respectively. Groundwater samples from the aquifers of the N-P system fall in an age bracket of modern–19 ka and modern–10 ka BP for Neogene aquifer and Paleogene aquifers, respectively. The oldest age (12–19 ka) groundwater of these aquifers occurs near Hanshuiquan area, except No. S15 (16 ka), between the two faults F1 and F2 without hydraulic connection with most samples in the basin.

Mechanism of recharge to aquifers

Sources of recharge to aquifers

The sources of recharge to aquifers can be traced by the stable isotope signature of waters. The δD–δ^{18}O plot of samples is shown in Fig. 3. It can be seen that the δ-values of samples were more negative than the weighted mean value of local precipitation. This finding indicates that the groundwater recharge source may not be dominated by the local precipitation within the basin, and the recharge water should come from high altitude or a cold climate.
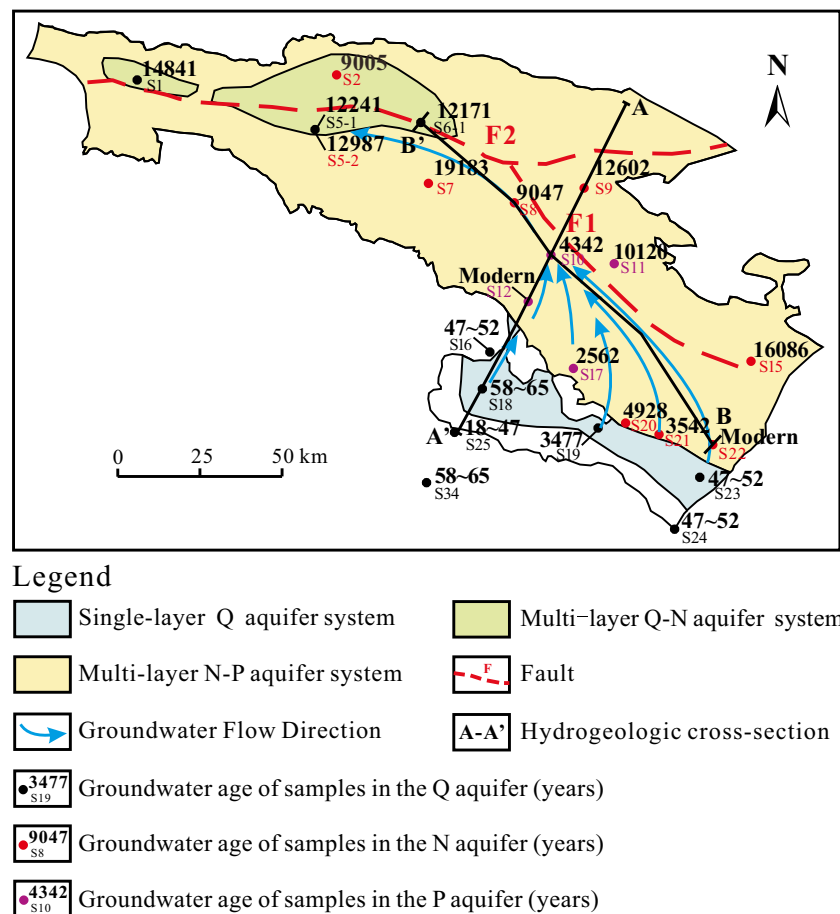
Fig. 7 The mean ^{14}C age distribution of groundwater. "Modern" here means groundwater recharged after 1950s

Tritium is a reliable indicator to distinguish modern recharge from pre-bomb recharge water. Samples that contained considerable tritium were found for groundwaters emerging in the single-layer system. This indicates that modern recharge mainly occurs in the piedmont of mountains. The samples of the single-layer system show two groups in the δD–δ^{18}O plot. Sample Nos. S26 and S19 plotted on the RRWL, and had the same isotopic signature as surface waters, which means these groundwaters were recharged by rivers without significant evaporation. Other samples deviated from the RRWL, indicating the effect of evaporation. The line fitted by those deviated samples (except for Nos. S19, S25 and S26) is $Y = 5.15X - 26.69$ and may represent the evaporation line. Sample S25 showed a high delta-value and largely deviated from the samples in the single layer system. In fact, S25 was sampled from a shallow dug well with a diameter of about 6 m and possibly represented the mixture of groundwater and local rain water, which was different from the groundwater of the single layer system and river water from the mountains. Interestingly, the S25 sample is located on the fitted line, indicating the evaporation effect. Generally, the extrapolated evaporation line and meteoric water line have an intersection point, and that point's isotope composition could represent the signature of the

original recharge water (Clark and Fritz 1997). The δD and δ^{18}O values at the intersection of the evaporation line with RRWL are −127.34 and − 19.54‰, respectively. The δ^{18}O value of this original recharge water is about 8.7‰ lower than the weighted mean value of local precipitation. This indicates that the recharge source is the precipitation of the high mountain areas. Gu and Longinelli (1993) derived a vertical gradient of 0.4‰/100 m by the isotopic studies on precipitation in the area above the snow line in the Tien Shan Mts. Thus, the mean altitude of source water estimated by this gradient is about 2,200 m, indicating that the dominated source of modern recharge to the aquifers is the precipitation of the mountain areas.

Groundwaters in Paleogene and Neogene aquifers should be pre-1950s recharge water because they are tritium free. Expect for three samples (Nos. S9, S11, S15), the stable isotopic composition of samples from the Neogene and Paleogene aquifers of the N-P system and the Neogene aquifer of the Q-N system show two narrow ranges of δD and δ^{18}O values and plot closer to the meteoric water line. The former data tend to be considerably more negative than the latter data. The isotopic ratios of both groups are more negative than the ratio of the mean annual rainfall. These data lie on a fitted line
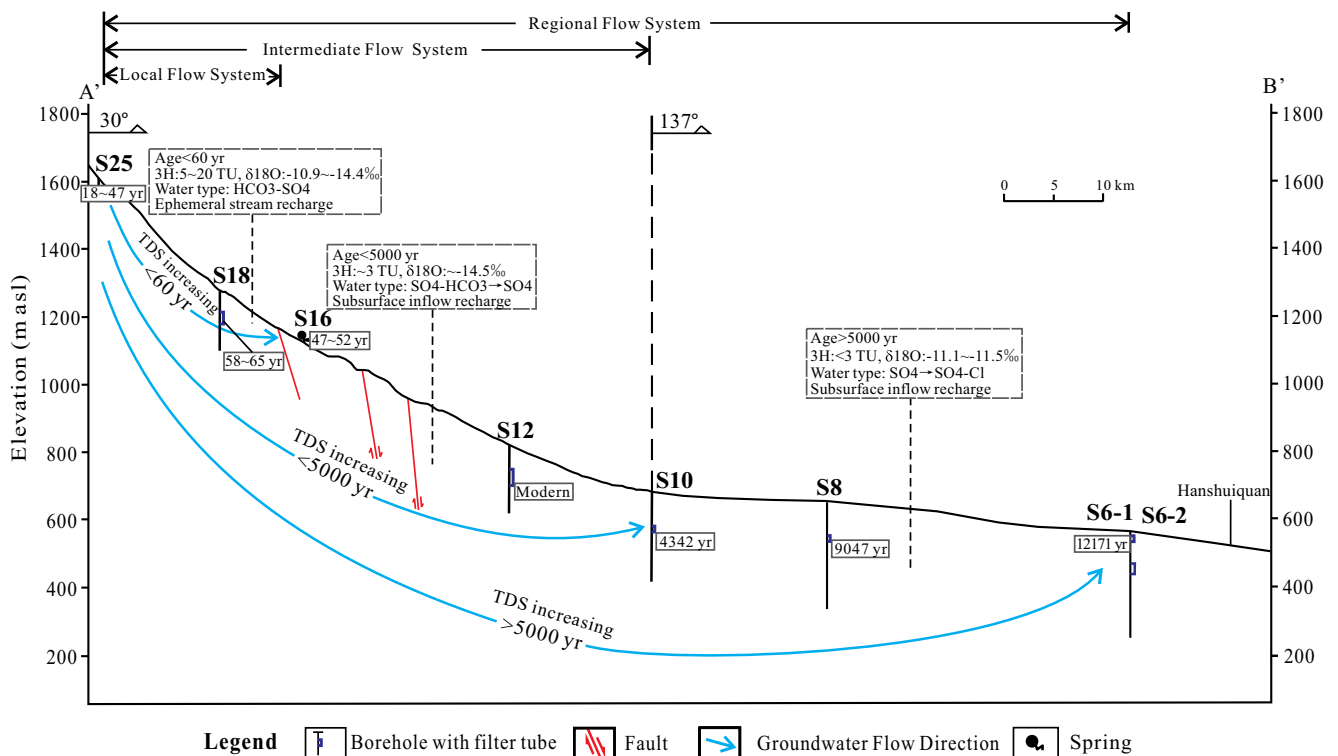
Fig. 8 Flow paths of groundwater flow systems along the transect A′–B′

to the right and are approximately parallel to the LMWL, indicating that recharge to the aquifer occurred during a climate that was both wetter and cooler than the present climate in the respective recharge areas. This explanation was supported by Li et al. (2015). The ^{14}C age of these samples ranges from a few thousand to more than 10,000 years and indicates they were palaeo-recharge waters.

Recharge mechanism

The stable isotopes of water have been shown to be particularly useful not only in tracing the sources of recharge water but also in distinguishing different recharge mechanisms. The stable isotope data of the water samples indicate two predominant recharge mechanisms that occur in the study area are: (1) ephemeral stream recharge, and (2) subsurface inflow recharge.

The ephemeral stream recharge is the recharge that results from the infiltration of ephemeral streams near the mountain front. In times of snowmelt and high rainfall events, ephemeral creeks are developed by surface-water run-off from the mountains and infiltrate through the highly permeable river bed deposits. There is evidence to suggest that this recharge is occurring today in the piedmont area and the most compelling evidence comes from the rivers region in the piedmont of Moqinwula Mts., i.e. the area of the single-layer aquifer system. As discussed previously, the samples with considerable tritium content represent recently recharged water, and they

plotted to the right of the RRWL along an evaporation line of slope = 5.15 in the δD–δ^{18}O plot. The signature of the original water suggested that the source of recharge water is from the mountain areas. Thus, these young groundwaters are assumed to be recharged by the infiltration of ephemeral streams with the occurrence of evaporation during recharge. It is also possible that ephemeral stream recharge occurs along a number of creeks along the piedmont of Baiyi Mts. and the north mountains. Unfortunately, there are no available isotopic data from these regions to support this.

The subsurface inflow recharge is defined as the recharge of subsurface water that moves laterally from mountain regions or an aquifer to adjacent aquifers. Such recharge is often an important recharge mechanism in semi-arid and arid catchments. One of the evidences for this mechanism is from the isotopic signature of sample Nos. S19 and S26. Both samples have similar stable isotopic signatures to river water samples Nos. S31 and S27, respectively. They plotted on the RRWL, indicating that they were not affected by evaporation. Two recharge processes may cause this. One is the rapid infiltration of ephemeral stream water through fractures or a highly permeable zone. And the other possible scenario is lateral subsurface inflow from the mountain block. If the former process takes place, groundwater should be recently recharged water with significant tritium content; thus, the sample No. S26 represents the former process, and sample No. S19 should be recharged by the latter process since it contains tritium less than 3 TU and ^{14}C < 80 pMC. Another similar situation could

be found for the N-P aquifer system. The samples Nos. S12 and S17 had similar δ values to Nos. S16 and S18, and the δ values of the samples Nos. S15, S20, S21, S22 were identical to those of Nos. S23, S24. This finding suggested that these groundwaters were recharged from the lateral subsurface inflow from the upstream single-layer aquifer system.

Flow path of regional flow system

Groundwater age can be used to identify the groundwater system and delineate the flow path of the regional flow system. The age data of samples indicate that both local and regional flow systems are present at the study area. The young groundwaters (<60 years) represent the short flow path associated with local flow systems, while the old groundwaters with residence >3,000 years reflect long flow paths associated with the intermediate or regional flow system. As shown in Fig. 6a, the local flow system occurs in the shallow part of the piedmont area with residence time < 60 years. Groundwaters in this system are HCO₃-SO₄ type with TDS <1,000 mg/L and their $\delta^{18}O$ values range from −10.9 (No. S25) to 14.4‰ (No. S16).

The deep flow system exists below the local system and groundwater age may be up to 4,342 years (No. S10). The $\delta^{18}O$ value of groundwaters is about −14.5‰ (Nos. S10, S12). The hydrochemistry changes from SO₄-HCO₃ to SO₄ type and TDS increases from <500 to ~1,100 mg/L with increasing groundwater age. This flow system might represent the intermediate flow system.

It should be noted that the $\delta^{18}O$ values of samples on the left side of the fault F1 are about −14.4 to −14.5‰, while the value of sample No. S9 on the right side of F1 is −10.0‰ (Fig. 6a). In addition, there is a significant difference in

hydrochemical characteristics between sample Nos. S9 and S10. This significant difference supports that the fault F1 is a relatively impermeable barrier to groundwater flow (Bai et al. 2015a). The importance of faults on controlling the groundwater flow path can be seen from the pattern of groundwater age (Fig. 7). Young groundwaters (Nos. S18, S23, S24) occur in the upgradient of the pluvial plain, and are modern recharged water with low TDS and HCO₃ or HCO₃-SO₄ type. Groundwaters of a few thousand years in age are found in the downgradient pluvial-alluvial plain (Nos. S17, S20, S21, S10). These indicate that modern recharged groundwater moves downgradient towards the north through lateral flow. An interesting finding is that the age of samples (S10, S8, S6–1, S5–1, S5–2) along the faults increases linearly from 4,230 years (No. S10) to more than 10,000 years. This suggests that the groundwater flow from the piedmont area has changed flow direction to the spring zone of Hanshuiquan Oasis along the faults due to the fault barrier, and developed a regional flow system.

This regional flow system can be identified from the transect along the faults (B–B′ in Fig. 6b). Groundwater is of modern age at the east end of B–B′, and age gradually increases westward to 12.2 ka (No. S6-1). The water type evolves from SO₄-HCO₃ to SO₄-Cl type, and TDS increases from ~500 (No. S22) to ~4,400 mg/L (No. S6-2) with increasing groundwater age. These results clearly indicate that the central faults are controlling the flow path of the regional groundwater flow system.

The groundwater flow systems and recharge mechanisms discussed in the preceding are summarized and illustrated in Figs. 8 and 9. The transect in Fig. 8 consists of two parts, to delineate the movement of groundwater from the piedmont
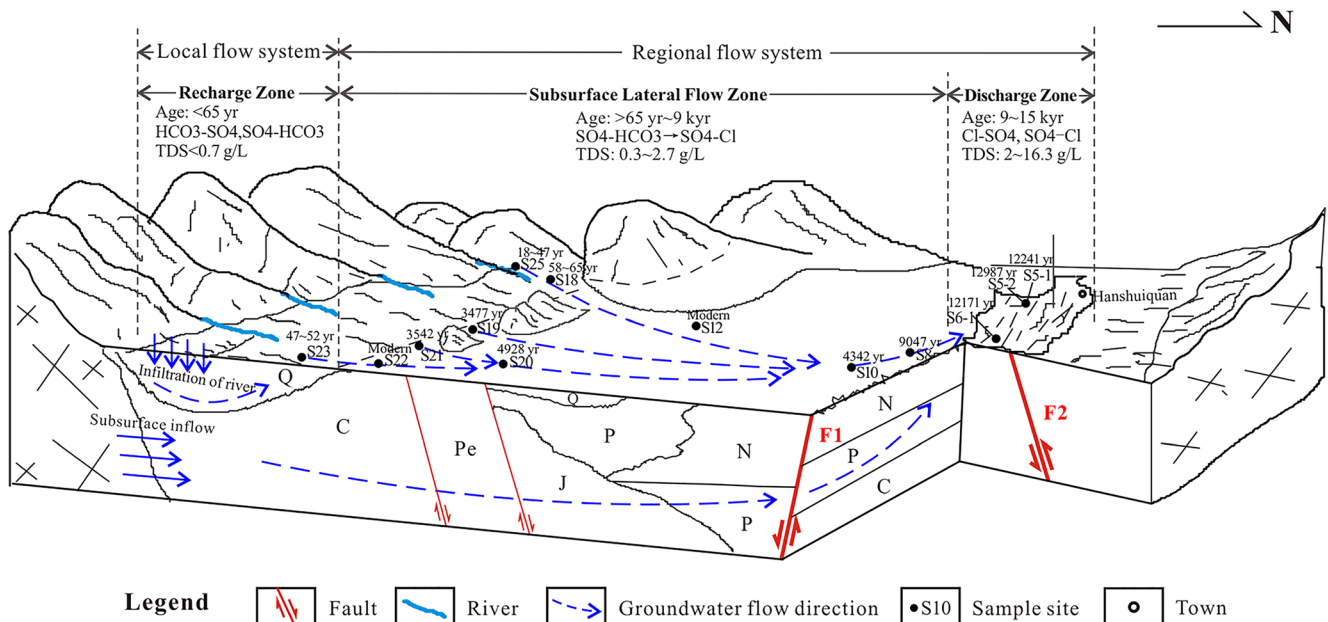

Fig. 9 Conceptual model of the recharge and groundwater flow in the basin

area to the discharge area: the south part of transect A′–A and the west part of B′–B. The local flow systems occur in the piedmont area with the circulation depth of less than 150 m. Groundwater is HCO$_3$-SO$_4$ type with TDS <1,000 mg/L and recharged by the infiltration of ephemeral streams in the foothills, and discharged as springs at the distal zone of the alluvial fan. The residence time of the groundwaters is from a few years to about 65 years.

The intermediate flow systems occur below the local flow systems, which may extend horizontally to the centre of the basin and finally depends upon the occurrence of faults. Groundwater is recharged by the subsurface inflow from the piedmont area and discharged by lateral outflow or upward leakage to the upper aquifer. Water type evolves from SO$_4$-HCO$_3$ in the upgradient part to SO$_4$ type in the downgradient accompanied by increasing of TDS. The age of groundwater in this system is no more than 5,000 years.

The regional flow systems occur in the deep confined aquifers, and they can achieve a thickness of several hundred meters. Groundwater is recharged by subsurface inflow and laterally moves from the piedmont plain to the lowland, and it changes flow direction nearly to the west, and finally discharges by upwards leakage or spring at the spring zone of Hanshuiquan Oasis. Water type evolves from SO$_4$ (No. S10) to SO$_4$-Cl type (Nos. S8, S6-2) with increasing TDS along the flow path. The age of groundwater in this system is more than 5,000 years.

Conclusions

The combination of age dating with hydrogeological information, hydrochemistry and isotope methodology provides a very valid and clear understanding of groundwater recharge and flow paths in the Santanghu basin. The main conclusions are:

1. Groundwater age is less than 65 years in the aquifer of the single-layer system, about 9–15 ka in the Quaternary–Neogene aquifer system, and up to ~19 ka in the Neogene-Paleogene aquifer system.
2. The dominant source of recharge to aquifers is the precipitation of the mountain areas with the mean altitude of about 2,200 m. The recharge took place by two recharge mechanisms: ephemeral stream recharge in the piedmont, and subsurface inflow recharge from the mountain region or adjacent aquifers. Diffuse recharge derived from precipitation in the basin can be ignored because of the scarcity of precipitation and intense evaporation.
3. The significant differences in the δ^{18}O values, ^{14}C age and hydrochemical characteristics between samples on both sides of the faults suggest that the faults could block groundwater flow. The pattern of groundwater age and the

evolution of hydrochemical characteristics indicate that the faults control the occurrence of the groundwater flow systems and the regional flow paths. The development of intermediate and regional flow systems depends upon the central faults. Groundwater moves from the piedmont area to the lowland area and changes flow direction towards the discharge zone of Hanshuiquan Oasis along the water-blocking fault in the centre of the basin.

References

Abbott MD, Lini A, Bierman PR (2000) δ^{18}O, δD and ^{3}H measurements constrain groundwater recharge patterns in an upland fractured bedrock aquifer, Vermont, USA. J Hydrol 228(1):101–112

Bai M, Li XX, Zhang J, Ju MT (2015a) An analysis of the control factors of groundwater storage in the Santanghu Basin of Xinjiang (in Chinese). Hydrogeol Geol 42(2):47–52

Bai M, Zhang J, Li XX, Ju MT (2015b) Distribution characteristics of groundwater storage in Santanghu Basin of Balikun County, Xinjiang (in Chinese). Xinjiang Geol 33(2):270–274

Bajjali W (2006) Recharge mechanism and hydrochemistry evaluation of groundwater in the Nuaimeh area, Jordan, using environmental isotope techniques. Hydrogeol J 14(1–2):180–191

Bourke SA, Cook PG, Dogramaci S, Kipfere R (2015) Partitioning sources of recharge in environments with groundwater recirculation using carbon-14 and CFC-12. J Hydrol 525:418–428

Chen X, Huang YY, Ling MH, Hu Q, Liu B (2012) Numerical modeling groundwater recharge and its implication in water cycles of two interdunal valleys in the Sand Hills of Nebraska. Phys Chem Earth 53:10–18

Chen ZL, Liu J, Gong HL, Han FB, Briggs SM, Zheng EJ, Wang G (2011) Late Cenozoic tectonic activity and its significance in the northern Junggar Basin, northwestern China. Tectonophysics 497(1):45–56

Chen ZY, Nie ZL, Zhang ZJ, Qi JX, Nan YJ (2005) Isotopes and sustainability of ground water resources, North China plain. Groundwater 43(4):485–493

Clark ID, Fritz P (1997) Environmental isotopes in hydrogeology, vol 328. CRC, New York

Doney SC, Glover DM, Jenkins WJ (1992) A model function of the global bomb tritium distribution in precipitation, 1960–1986. J Geophys Res 97(C4):5481–5492

Edmunds WM, Ma JZ, Aeschbach-Hertig W, Kipfer R, Darbyshire DPF (2006) Groundwater recharge history and hydrogeochemical evolution in the Minqin Basin, North West China. Appl Geochem 21(12):2148–2170

Gates JB, Edmunds WM, Ma JZ, Scanlon BR (2008) Estimating groundwater recharge in a cold desert environment in northern China using chloride. Hydrogeol J 16(5):893–910

Gu WZ, Longinelli A (1993) A case study on the hydrological significance of stable isotope data on Alpine catchments with snow cover and glaciers, Xinjiang, China. Snow Glacier Hydrol 218:371–383

Kreutz KJ, Wake CP, Aizen VB, Cecil LD, Synal HA (2003) Seasonal deuterium excess in a Tien Shan ice core: influence of moisture transport and recycling in Central Asia. Geophys Res Lett 30(18): 1922

Li J, Pang ZH, Froehlich K, Huang TM, Kong YL, Song WH, Yun HX (2015) Paleo-environment from isotopes and hydrochemistry of groundwater in east Junggar Basin, Northwest China. J Hydrol 529:650–661

Ma JZ, He JH, Qi S, Zhu GF, Zhao W, Edmunds WM, Zhao YP (2013) Groundwater recharge and evolution in the Dunhuang Basin, northwestern China. Appl Geochem 28:19–31

Małoszewski P, Zuber A (1982) Determining the turnover time of groundwater systems with the aid of environmental tracers: 1. models and their applicability. J Hydrol 57(3–4):207–231

Pearson FJ, Hanshaw BB (1970) Sources of dissolved carbonate species in groundwater and their effects on carbon-14 dating. In: IAEA (ed) Isotope hydrology 1970. IAEA, Vienna, pp 271–285

Scanlon BR, Healy RW, Cook PG (2002) Choosing appropriate techniques for quantifying groundwater recharge. Hydrogeol J 10(1): 18–39

Sophocleous M (2005) Groundwater recharge and sustainability in the High Plains aquifer in Kansas, USA. Hydrogeol J 13(2):351–365

Tamers MA (1975) Validity of radiocarbon dates on ground water. Geophys Surv 2:217–239

Verhagen BT, Mazor E, Sellshop JPF (1974) Radiocarbon and tritium evidence for direct recharge to groundwaters in the northern Kalahari. Nature 249:643–644

Vogel JC (1970) Carbon-14 dating of groundwater. In: Isotope hydrology. IAEA, Vienna, pp 225–239

Zagana E, Obeidat M, Kuells C, Udluft P (2007) Chloride, hydrochemical and isotope methods of groundwater recharge estimation in eastern Mediterranean areas: a case study in Jordan. Hydrol Process 21(16):2112–2123

Zhang L, Chen ZY, Nie ZL, Liu FL, Jia YK, Zhang XY (2008) Correlation between δ^{18}O in precipitation and surface air temperature on different time-scales in China (in Chinese). Nucl Tech 31(9): 715–720